Supporting Information for

Graphene/Polyurethane Nanocomposites for Improved Gas Barrier and Electrical Conductivity

Hyunwoo Kim, Yutaka Miura and Christopher W. Macosko

Department of Chemical Engineering and Materials Science, University of Minnesota,

Minneapolis, Minnesota 55455-0331

Supporting Information 1: X-ray photoelectron spectrum of graphitic derivatives

X-ray photoelectron spectra (XPS) of graphite, graphite oxide (GO), phenyl isocyanate treated GO (Ph-iGO) and thermally reduced GO (TRG) were collected with a Physical Electronic model 555 spectrometer with MgKα radiation (accelerating voltage of 12 kV at 250 W). Three sweeps were averaged for a survey scan with pass energy of 200 eV. Higher resolution spectra at the C_{1s} level were also obtained with pass energy of 25 eV.

In the XPS survey scans (Figure SI1 (a)), notable reflections at binding energy of ~ 169, 285, 402 and 533 eV correspond to S_{2p}, C_{1s}, N_{1s} and O_{1s} levels, respectively.[1] Integration of the XPS intensity at each level gave atomic concentrations in these graphitic derivatives. While a small amount of silicon was also detected (weak reflections at ~ 153 eV (Si_{2s}) and 101 eV (Si_{2p})), it was not included for the atomic composition estimation. For high-resolution C_{1s} XPS (Figure SI1 (b)), intensities were scaled such that all spectra have the same area under the C_{1s} peak. The

symmetric C_{1s} spectrum of pristine graphite, centered at 284.5 eV, became asymmetric after oxidation, indicative of formation of carbon-oxygen bonds with higher binding energy.[2,3] TRG showed less asymmetry indicating that the rapid pyrolysis reduced oxygen content.[4]

Supporting Information 2. Raman spectroscopy of graphitic carbons

Raman spectroscopy was conducted on graphite, GO and TRG using a Witec Alpha300R confocal Raman microscope connected with a class III Argon laser source (Omnichrome, CA) with wavelength of 514.5 nm. Raman signal was integrated over 20 sec for each spectrum. In the Raman spectrum of graphite (Figure SI2), G band reflection at 1550-1650 cm^{-1} arising from vibration in sp^2-hybridized carbon domains[5] is strongest implying crystalline graphitic carbons are mainly intact. Oxidation not only diminishes the G band intensity but also intensifies the D band centered at 1350 cm^{-1} which is activated by defect-like amorphous carbons (sp^3-hybridization).[5] Incorporation of oxygen into graphene requires flat graphitic carbons to be displaced into out-of-plane geometry inducing sheet deformation.[4,6] The slightly enhanced G band of TRG may be accounted for by partial restoration of graphitic domains through "self-healing" during thermal reduction.[7,8]

Supporting Information 3: Graphene characterization with Fourier transform infrared spectroscopy

Fourier transform infrared (FTIR) spectra were obtained for graphite, GO, TRG, acetylphenyl isocyanate treated GO (AcPh-iGO) and GO separated from in-situ polymerized thermoplastic polyurethane (TPU) composites. Separation was conducted with Soxhlet extraction for 48 hrs using 1.5 mm-thick cellulose thimbles (Advantec, No. 84) and tetrahydrofuran (THF) boiling at 85 ^oC. Graphitic residues retained in the thimble were repeatedly washed with THF,

then dispersed in THF and centrifuged (CR 3-22, Jouan) for 10 min at 5000 RPM. Particles were dispersed in THF (0.5 mg/mL) and coated on KBr disks, followed by removal of THF in vacuo at 45 °C. FTIR spectra over the wavenumber range of 650-4000 cm^{-1} were obtained in a transmission mode with a Nicolet Magna-IR 750 spectrometer at a resolution of 2 cm^{-1}. During spectrum acquisition, samples were purged with dry N_2.

Infrared (IR) transmittance of each graphitic material in the range of 1000-2000 cm^{-1} is shown in Figure SI3 (a). Chemical changes of graphite upon oxidation, rapid pyrolysis and isocyanate functionalization can be detected by FTIR. Noticeable absorptions of GO are located at 1730 (C=O carbonyl or carboxyl stretching), 1620 (C-O-C or adsorbed H_2O deformation vibration), 1230 (C-OH stretching) and 1050 cm^{-1} (skeletal C-O or C-C stretching).[2,9-11] The broad reflection at ~ 1400 cm^{-1} originates from O-H deformation and C-OH vibration. After graphite oxidation, a broad band at 3000-3700 cm^{-1} also appears in the IR spectrum (Figure SI3 (b)), which signifies stretching vibration of surface hydroxyls (~ 3400) and water absorption (~ 3200 cm^{-1}).[10-12]

The spectrum for TRG lacks reflections from C=O and C-O stretching at 1000-2000 cm^{-1} suggesting loss of oxygen during thermal treatments. However, the hydroxyl and H_2O stretching band at 3000-3700 cm^{-1} is still observed, which indicates some functionalities are still present. After treating GO with acetylphenyl isocyanate, absorption bands were shifted to 1700, 1650 (C=O stretching in carbamate esters and amide groups, respectively) and 1540 cm^{-1} (vibration of CNH groups) which all are associated with carbamate and amide formation.[12,13] Although only appearing as shoulders to the stronger reflections, GO recovered from in-situ polymerized composites has analogous IR features to carbamate and TPU, which are indicative of grafting of TPU chains on GO via urethane or amide linkages during polymerization. Possible complication

by physi-sorption of TPU on GO surface should be excluded since the supernatant portion after the centrifugation of THF containing Soxhlet-extracted GO did not display any features related to TPU, confirming complete removal of free TPU chains with repeated washing. Besides these reflections, strong C-H stretching absorptions at 2850-3000 cm^{-1} (Figure SI3 (b)) also corroborate the existence of alkyl chains on GO surfaces.

Supporting Information 4: Synthesis and molecular weights of in-situ polymerized TPU composites

TPU and its composites containing TRG or GO were polymerized from 4,4'-methylene diphenyl diisocyanate (MDI), ester-based polyol (Daltorez P765, Huntsman Polyurethanes) and 1,4-butanedial (BDO). Weight and molar ratios of each component used in in-situ polymerization of the composites are summarized in Table SI4. Note that MDI was used in 0.2 - 5% excess from the stoichiometric ratio to compensate for consumption of isocyanate groups by moisture and –OH groups on TRG or GO surface, and to prevent significant molecular weight reduction.

Number (M_n) and weight (M_w) average molecular weights of Avalon 70AE and in-situ polymerized TPU were determined with size exclusion chromatography (SEC, Waters 717 Plus HPLC Autosampler) at room temperature using THF as a mobile phase and polystyrene standards (EasiCal PS-2, Polymer Laboratories). Before running SEC, the TPU matrix was separated from the in-situ polymerized composites by Soxhlet extraction for 48 hrs using THF at 85 ^{o}C. Separation continued by centrifugation of the extracted matrix in THF for 10 min at 5000 RPM and only the supernatant portion was collected for SEC.

For some in-situ polymerized samples, shoulders appeared toward smaller retention time in the SEC traces (Figure SI4). These asymmetric SEC traces were deconvoluted to yield two Gaussian distributions and the one located at lower retention time was not included for calculating the M_w and M_n values reported in Table SI4. The shoulders located at lower retention time are presumably due to a fraction of TRG particles extracted along with TPU and suspended in the THF mobile phase even after centrifugation. TRG diameter[14] ranges from 50 to 400 nm, which means the radius of gyration of smaller particles can be comparable with that of typical polymer chains[15] especially if these thin flexible membranes adopt a "crumpled sphere" configuration in solvents.[16]

Molecular weights of TPU polymerized in *N,N*-dimethylformamide (DMF) without TRG or GO are slightly lower than those of Avalon 70AE (96,000 (M_w) and 55,000 g/mol (M_n)), but are significantly higher than those of the pre-polymer collected before the chain extension reaction (10,000-11,000 (M_w) and 5,000-7,000 g/mol (M_n)). TPU extracted from the TRG and GO in-situ polymerized samples has both lower and higher molecular weights. These differences are most likely due to a combination of isocyanate consumption by TRG or GO and errors in peak deconvolution.

Supporting Information 5. Tensile modulus data of graphene/TPU composites

Table SI5 summarizes tensile modulus data of TPU composites. The average modulus measured for 3-4 samples and their standard deviation are reported. Sample to sample variation in modulus is relatively small confirming measurements are well reproduced. Except for a few samples, standard deviation is less than 10% of modulus. Standard deviation is ~ 5% of modulus on average.

Supporting Information 6: Dynamic mechanical analysis of TPU composites

Thermo-mechanical properties of TPU composites were studied with a dynamic temperature ramp (-60 to 150 ^{o}C at a rate of 3 ^{o}C/min) using Rheometrics Solids Analyzer II (RSA II). 3 mm wide and 0.1 mm thick strips cut from the cast films were dried in vacuo at room temperature and mounted between film fixtures of RSA II. Dynamic tensile storage *E'* and loss moduli *E"* were measured at 1 rad/s. During each test, static pretension on the specimens was maintained at about 200% of the dynamic forces which were kept between 0.2 and 1.0 N using auto-tension and auto-strain adjustments. Soft segment glass transition temperature $T_{g,\,soft}$ was estimated from the temperature at maximum tan δ (=*E"*/*E'*).

E', *E"* and tan δ of solvent blended and in-situ polymerized composites as a function of temperature are compared in Figure SI6. *E'* of all samples decreases drastically and tan δ reaches maximum at ~ -30 °C signifying softening of TPU at $T_{g,\,soft}$. Dispersion of TRG or GO improves TPU modulus, most significantly in the rubbery plateau region. Less pronounced modulus enhancements below $T_{g,\,soft}$ can be attributed to higher matrix modulus which undercuts stiffness contrast between matrix and reinforcement phase. In case of solvent blended samples (Figure SI6 (a) and (b)), there are no noticeable changes by TRG addition in $T_{g,\,soft}$, tan δ and the relaxation behaviors originating from hard domain dissociation above 100 °C. However, for in-situ polymerized samples, TRG (Figure SI6 (c) and (d)) or GO (Figure SI6 (e) and (f)) dispersion increased $T_{g,\,soft}$ by 3-7 °C. As well as higher $T_{g,\,soft}$, 0.5 wt% TRG or GO composites exhibit higher tan δ than neat TPU reflecting increased polyurethane inter-domain mixing.[17] Less significant increase in rubbery plateau modulus by TRG or GO incorporation may also be attributed to reduction in matrix modulus by the phase-mixing in TPU. However, the maximum

tan δ for composites containing higher fraction of TRG and GO (2.7-2.8 wt%) is smaller than that of TPU due to enhanced rubbery modulus. Interestingly, *E'* of in-situ polymerized samples does not decline at 110 ~ 120 °C as precipitously as that of solvent mixed ones. Appearance of another *E'* plateau at ~ 150 °C for TRG composites (Figure SI6 (c)) suggests mechanical relaxation is suppressed up to higher temperature. One possible origin of the extended rubbery plateau is formation of networks that do not thermally dissociate at 100 ~ 150 °C via TPU chains grafted on TRG surface.

Supporting Information 7: Mori-Tanaka's model for composite tensile moduli and material parameters

Tandon and Weng[18] derived an analytical formula from the model of Mori and Tanaka[19] for transverse modulus E_{11} of composites containing mono-dispersed ellipsoids with perfect planar orientation,

$$\frac{E_{11}}{E_m} = \frac{1}{1+\phi(-2\nu_m A_3 + (1-\nu_m)A_4 + (1+\nu_m)A_5 A)/2A}$$

where ϕ, E_m and ν_m are volume fraction of the reinforcing inclusions, Young's modulus and Poisson's ratio of the matrix, respectively. A and A_i are functions of ϕ, ν_m and components of Eshelby's tensor,[20,21] the detailed formula for which can be found in Tandon and Weng. In modeling of modulus increase by graphene addition, E_{TPU} was assumed to be 6.1 and 6.6 MPa for melt and solvent processed Avalon 70AE, and 7.2 MPa for in-situ polymerized TPU as determined experimentally. Both theoretical prediction[22] and experimental measurements[23] estimate the in-plane modulus of graphene E_{graphite} ~ 1060 GPa. For the matrix Poisson's ratio,

ν_{TPU} = 0.48 considering small matrix compressibility for elastomers[24] and for graphene, $\nu_{graphene}$ = 0.006, the Poisson's ratio reported for graphite.[25]

Supporting Information 8: Ultimate mechanical properties of TPU composites

Ultimate mechanical properties (e.g. strain at break, tensile strength and toughness) were measured by stretching ~ 4 mm wide composite films at a constant rate (0.024 /s) until fracture using a Polymer Laboratories Minimat. Representative stress-strain responses of TPU composites are shown in Figure SI8. Most rigid fillers increase modulus, but significantly reduce elongation. However, addition of graphene does not notably influence the strain at break of TPU. Note that TRG dispersion leads to decrease in tensile strength for solvent blended samples (Figure SI8 (a)), while the strength increases for in-situ polymerized ones (Figure SI8 (c)). Toughness (area under stress-strain curves) of solvent blended TPU/TRG composites is slightly improved at 0.5 wt% TRG, but subsequently decreases at higher loadings. In case of Ph-iGO (Figure SI8 (b)), composite films all fractured at higher elongation than un-filled TPU. Tensile behavior of composites in-situ polymerized with TRG or GO (Figure SI8 (c) and (d)) is distinctive compared with solvent blended ones. The ultimate strength of the TPU alone is lower than the commercial Avalon 70AE sample, 14 MPa versus 22 MPa. Unlike neat in-situ polymerized TPU, composites polymerized with small incorporation of TRG or GO show strain hardening around 500% strain in their stress-strain responses resulting in significantly enhanced tensile strength. Higher soft-hard domain mixing[17] and surface grafting with TPU could play a role. However, higher amount (2.7 ~ 2.8 wt%) of TRG and GO did not improve the strength as significantly, possibly owing to excessive decrease in inter-chain hydrogen bonding or matrix molecular weight reduction.

Supporting Information References

(1) NIST X-ray Photoelectron Spectroscopy Database, http://srdata.nist.gov/xps/Default.aspx, Accessed April 30, 2010.

(2) Hontoria-Lucas, C.; Lopez-Peinado, A. J.; Lopez-Gonzalez, J. d. D.; Rojas-Cervantes, M. L.; Martin-Aranda, R. M. *Carbon* **1995**, *33*, 1585-92.

(3) Stankovich, S.; Dikin, D. A.; Piner, R. D.; Kohlhaas, K. A.; Kleinhammes, A.; Jia, Y.; Wu, Y.; Nguyen, S. T.; Ruoff, R. S. *Carbon* **2007**, *45*, 1558-1565.

(4) Schniepp, H. C.; Li, J.-L.; McAllister, M. J.; Sai, H.; Herrera-Alonso, M.; Adamson, D. H.; Prud'homme, R. K.; Car, R.; Saville, D. A.; Aksay, I. A. *J. Phys. Chem. B* **2006**, *110*, 8535-8539.

(5) Tuinstra, F.; Koenig, J. L. *J. Chem. Phys.* **1970**, *53*, 1126-30.

(6) Li, J.-L.; Kudin, K. N.; McAllister, M. J.; Prud'homme, R. K.; Aksay, I. A.; Car, R. *Phys. Rev. Lett.* **2006**, *96*, 176101/1-176101/4.

(7) Kudin, K. N.; Ozbas, B.; Schniepp, H. C.; Prud'homme, R. K.; Aksay, I. A.; Car, R. *Nano Lett.* **2008**, *8*, 36-41.

(8) Yang, D.; Velamakanni, A.; Bozoklu, G.; Park, S.; Stoller, M.; Piner, R. D.; Stankovich, S.; Jung, I.; Field, D. A.; Ventrice, C. A., Jr.; Ruoff, R. S. *Carbon* **2009**, *47*, 145-152.

(9) Titelman, G. I.; Gelman, V.; Bron, S.; Khalfin, R. L.; Cohen, Y.; Bianco-Peled, H. *Carbon* **2005**, *43*, 641-649.

(10) Szabo, T.; Berkesi, O.; Dekany, I. *Carbon* **2005**, *43*, 3186-3189.

(11) Kovtyukhova, N. I.; Ollivier, P. J.; Martin, B. R.; Mallouk, T. E.; Chizhik, S. A.; Buzaneva, E. V.; Gorchinskiy, A. D. *Chem. Mater.* **1999**, *11*, 771-778.

(12) Stankovich, S.; Piner, R. D.; Nguyen, S. T.; Ruoff, R. S. *Carbon* **2006**, *44*, 3342-3347.

(13) Gunzler, H.; Gremlich, H.-U. *IR Spectroscopy*; Wiley-VSH: Winheim, 2002.

(14) Kim, H.; Macosko, C. W. *Macromolecules* **2008**, *41*, 3317-3327.

(15) Fractal dimension d_f of crumpled sheets can be 2.5 (good solvents) ~ 3.0 (poor solvents). This gives the radius of gyration ~ $(R^2 \cdot h)^{1/df}$ of 15 ~ 90 for good solvents and 10 ~ 40 nm for poor solvents assuming TRG diameter R = 25-200 nm and thickness ~ 1.8 nm (thickness of TRG).

(16) Wen, X.; Garland, C. W.; Hwa, T.; Kardar, M.; Kokufuta, E.; Li, Y.; Orkisz, M.; Tanaka, T. *Nature* **1992**, *355*, 426-8.

(17) Miller, J. A.; Lin, S. B.; Hwang, K. K. S.; Wu, K. S.; Gibson, P. E.; Cooper, S. L. *Macromolecules* **1985**, *18*, 32-44.

(18) Tandon, G. P.; Weng, G. J. *Polym. Compos.* **1984**, *5*, 327-333.

(19) Mori, T.; Tanaka, K. *Acta Metall.* **1973**, *21*, 571-574.

(20) Eshelby, J. D. *Proc. Roy. Soc. (London)* **1957**, *241*, 376-396.

(21) Eshelby, J. D. *Proc. Roy. Soc. (London)* **1959**, *252*, 561-569.

(22) Kelly, B. T. *Physics of Graphite*; 1st ed.; Applied Science: London, 1981.

(23) Lee, C.; Wei, X.; Kysar, J. W.; Hone, J. *Science* **2008**, *321*, 385-388.

(24) Qi, H. J.; Boyce, M. C. *Mech. Mater.* **2005**, *37*, 817-839.

(25) Cho, J.; Luo, J. J.; Daniel, I. M. *Compos. Sci. Technol.* **2007**, *67*, 2399-2407.

Table SI4. Weight and Molar Fractions of Components for TPU and Composite Synthesis and Matrix Molecular Weights

Sample	Weight fraction (%)				Mole fraction (%)			Molecular weight (kg/mol)		
	Reinforcement	Polyol	MDI	BDO	Polyol	MDI	BDO	M_w	M_n	PDI
TPU	0	73.3	21.9	4.8	19.1	50.2	30.7	68	39	1.7
TRG/TPU	0.5	73.0	21.8	4.7	19.2	50.5	30.3	57	27	2.1
	0.9	72.6	21.8	4.7	19.2	50.6	30.3	115	45	2.6
	2.7	71.1	21.5	4.7	19.0	50.7	30.2	103	39	2.6
GO/TPU	0.5	72.8	21.9	4.8	19.0	50.1	30.9	155	49	3.2
	0.9	71.2	23.4	4.5	18.4	53.4	28.2	90	53	1.7
	2.8	68.6	24.2	4.4	17.7	55.0	27.3	28	17	1.7

Table SI5. Tensile Modulus of Graphene/TPU Composites

Sample									
Blending method	Reinforcement	wt%	vol%	Tensile modulus (MPa)				Average (MPa)	Standard deviation
melt blend	graphite	0.0	0.0	5.5	6.7	6.1	-	6.1	0.5
		1.0	0.5	6.8	6.1	6.3	-	6.4	0.3
		3.0	1.6	9.0	8.5	8.4	-	8.7	0.2
		5.0	2.7	8.9	8.5	8.9	-	8.8	0.2
		15.0	8.6	21.4	25.3	20.8	-	22.5	2.0
	FGS	0.5	0.3	9.1	9.1	9.1	-	9.1	0.0
		1.0	0.5	11.5	-	-	-	11.5	-
		1.5	0.8	14.2	14.8	14.6	-	14.5	0.2
		2.0	1.1	15.2	15.3	15.8	16.5	15.7	0.5
		3.0	1.6	20.8	20.6	21.0	-	20.8	0.2
solvent blend	FGS	0.0	0.0	6.5	6.7	-	-	6.6	0.1
		0.5	0.3	12.5	14.4	13.1	-	13.3	0.8
		1.0	0.5	14.5	14.7	16.4	16.4	15.5	0.9
		3.0	1.6	52.8	53.4	53.5	-	53.2	0.3
	Ph-iGO	0.5	0.3	11.3	12.4	12.7	-	12.1	0.6
		1.0	0.5	17.7	20.1	18.1	-	18.6	1.0
		3.0	1.6	63.3	61.2	82.8	-	69.1	9.7
	AcPh-iGO	0.5	0.3	9.5	11.7	10.2	-	10.5	0.9
		1.0	0.5	16.7	21.3	20.7	-	19.6	2.0
		3.0	1.6	39.3	37.4	37.6	-	38.1	0.9
in-situ polymerized	FGS	0.0	0.0	8.0	6.9	6.7	-	7.2	0.5
		0.5	0.2	7.1	6.9	6.9	-	7.0	0.1
		0.9	0.5	10.3	10.8	13.4	12.1	11.7	1.2
		2.7	1.5	23.5	22.9	22.9	-	23.1	0.3
	GO	0.5	0.2	7.4	7.1	7.2	-	7.2	0.1
		0.9	0.5	9.0	10.6	9.7	-	9.8	0.6
		2.8	1.5	29.0	27.6	29.5	-	28.7	0.8

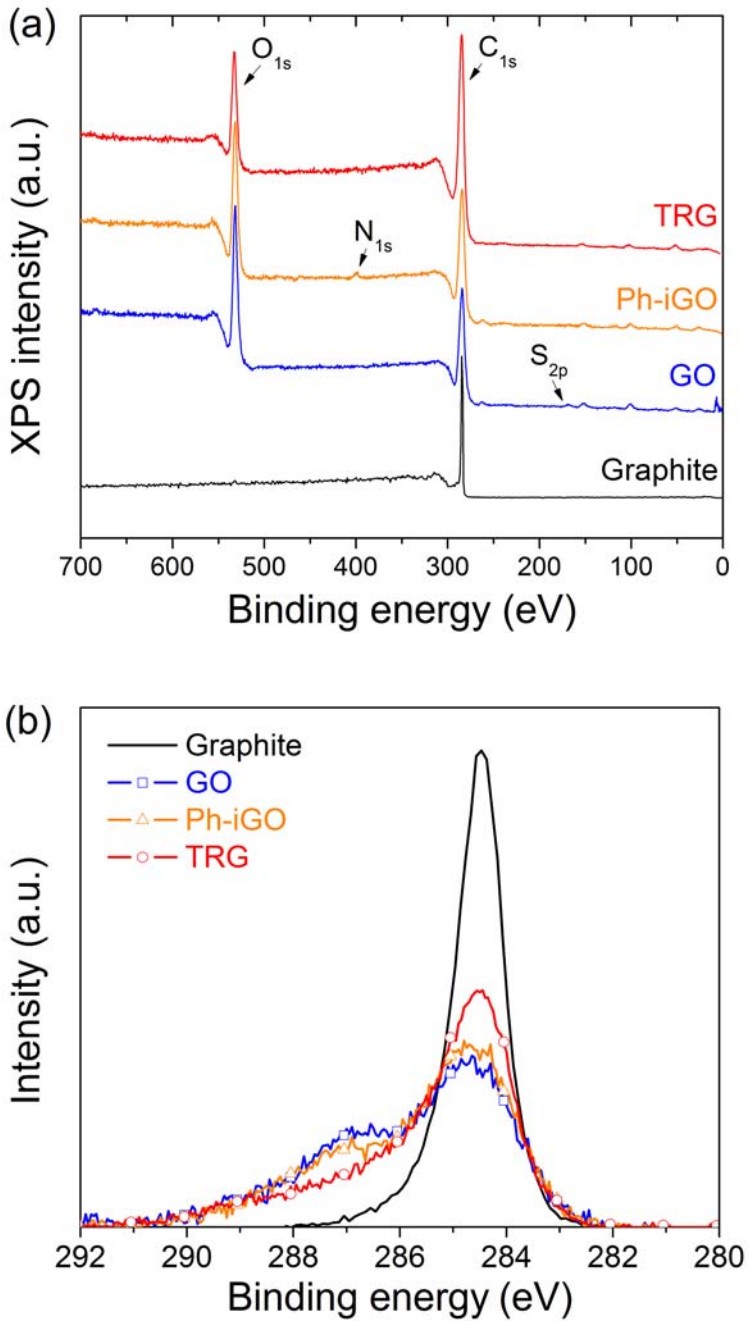

Figure SI1. (a) Survey XPS scans and (b) high-resolution C_{1s} spectra of graphite, GO, Ph-iGO and TRG. (a) Survey spectra were vertically shifted for clarity. (b) High-resolution C_{1s} peak intensities were adjusted for the same area under the peaks.

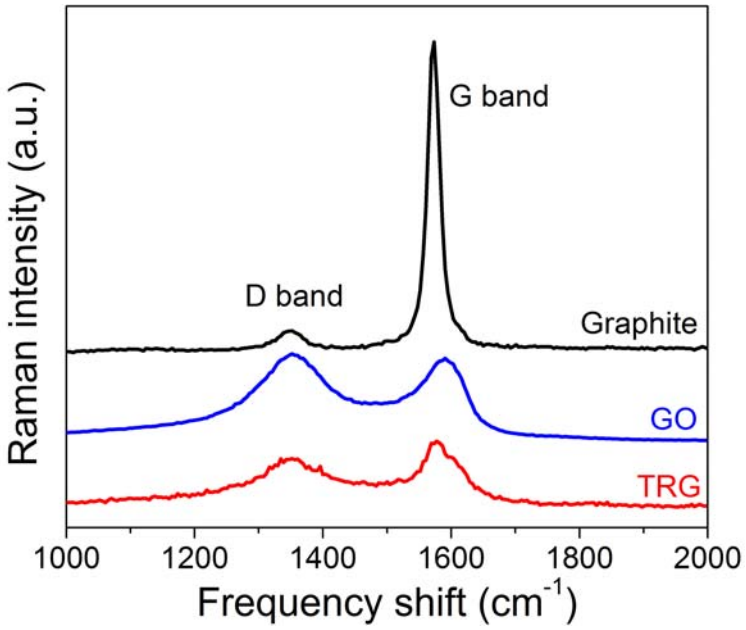

Figure SI2. Raman spectra of graphite, GO and TRG. Spectra were shifted vertically for clarity.

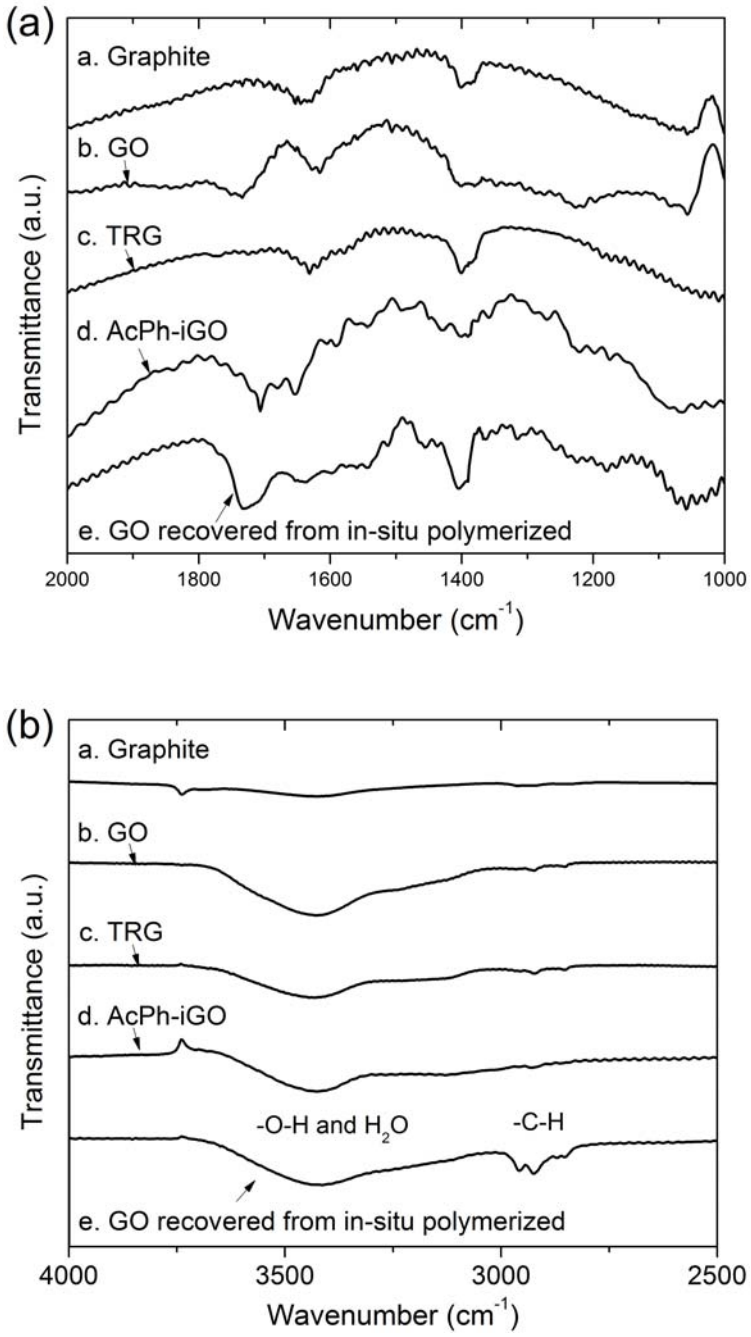

Figure SI3. FTIR spectra of a. graphite, b. GO, c. TRG, d. AcPh-iGO and e. GO recovered from in-situ polymerized TPU composites at (a) 1000-2000 and (b) 2500-4000 cm^{-1}. Spectra were shifted vertically for clarity.

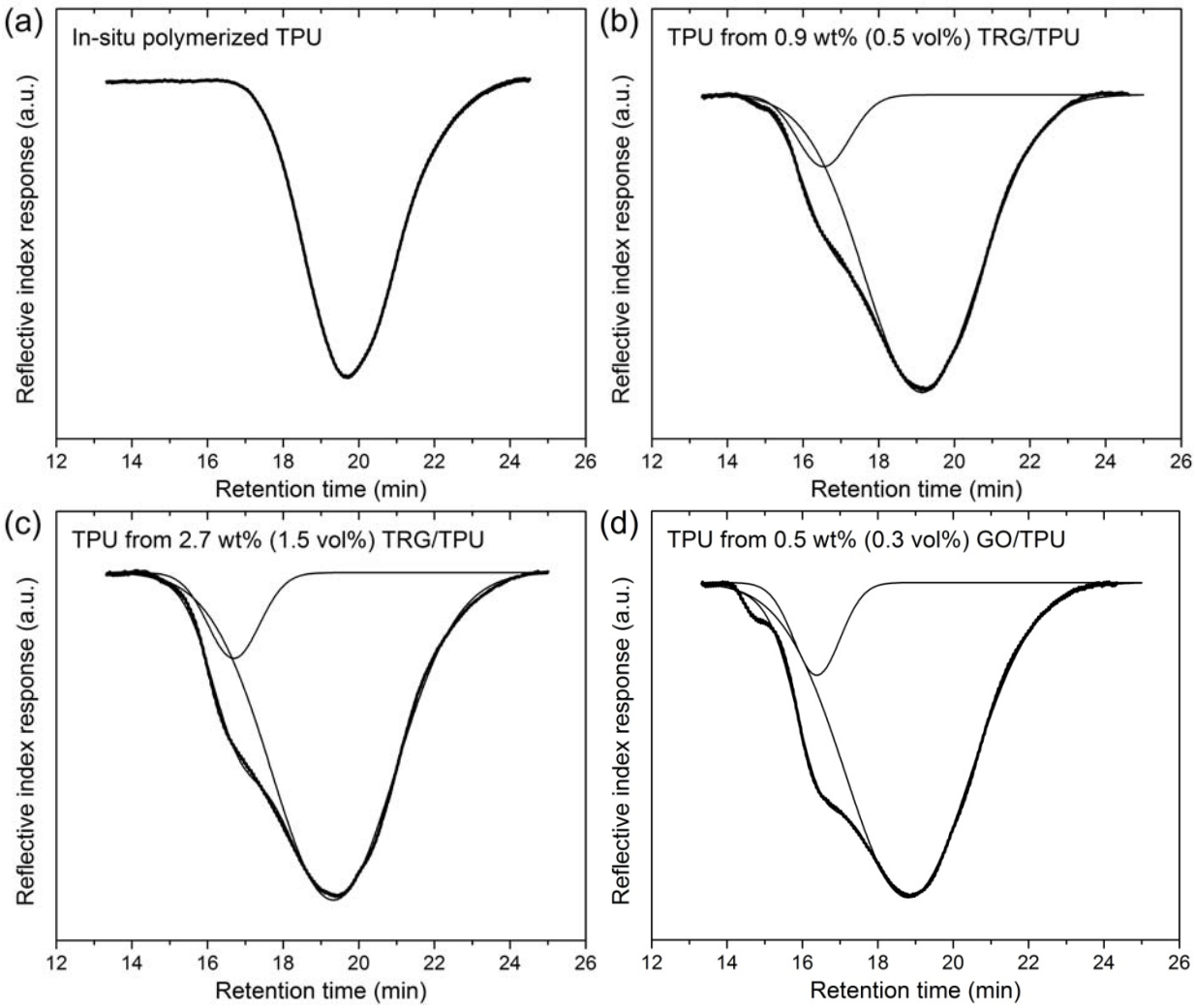

Figure SI4. SEC traces of (a) TPU in-situ polymerized, TPU extracted from in-situ polymerized (b) 0.9 wt%, (c) 2.7 wt% TRG and (d) 0.5 wt% GO/TPU composites. Peak deconvolutions based on the Gaussian distribution are also shown.

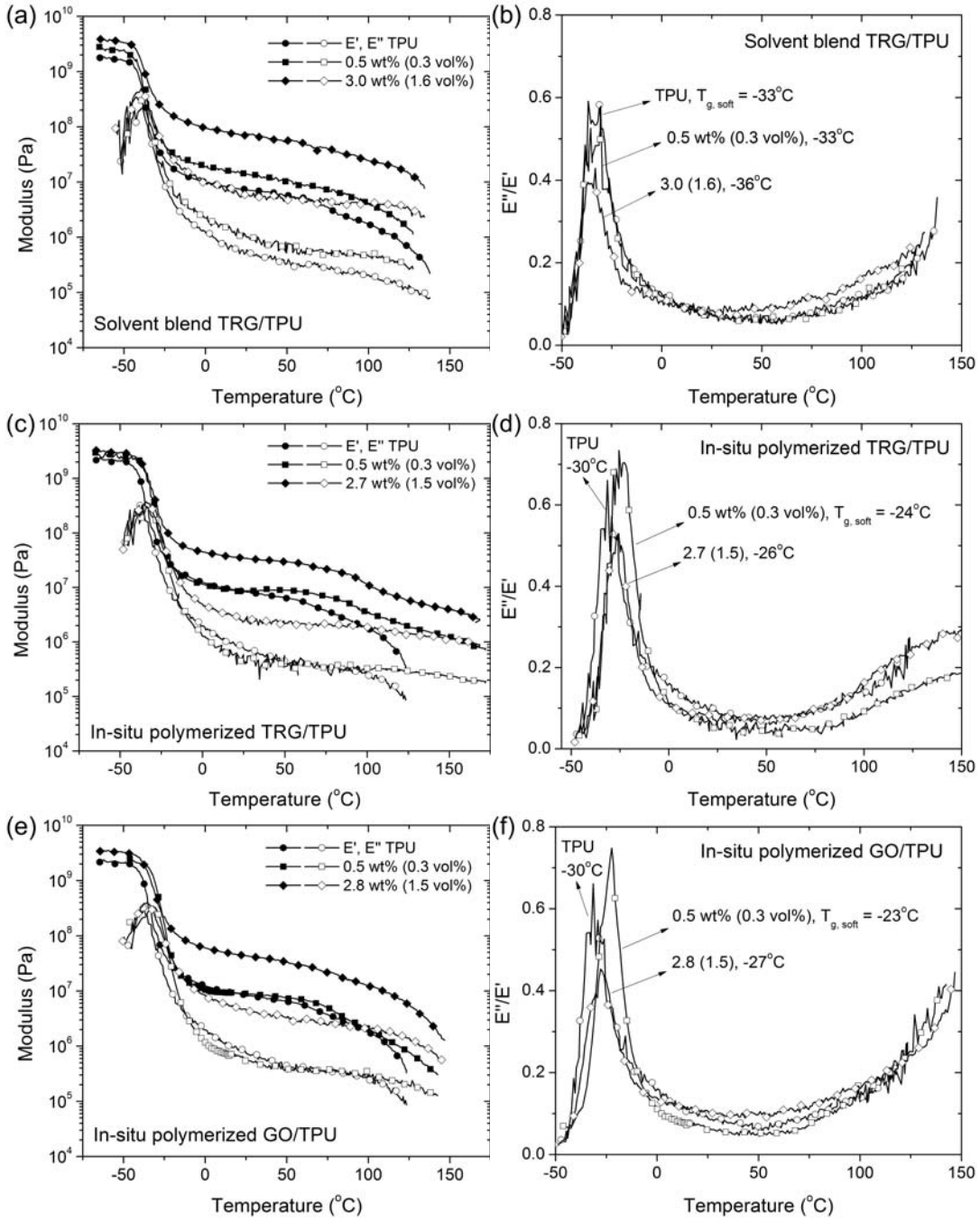

Figure SI6. Dynamic storage *E'* (closed) and loss modulus *E"* (open symbols), tan δ (*E''*/*E'*) changes with temperature for (a), (b) solvent blended TRG, (c), (d) in-situ polymerized TRG/TPU and (e), (f) in-situ polymerized GO/TPU composites. TPU soft segment glass transition temperature $T_{g,\,soft}$ determined from the maximum tan δ location is also shown.

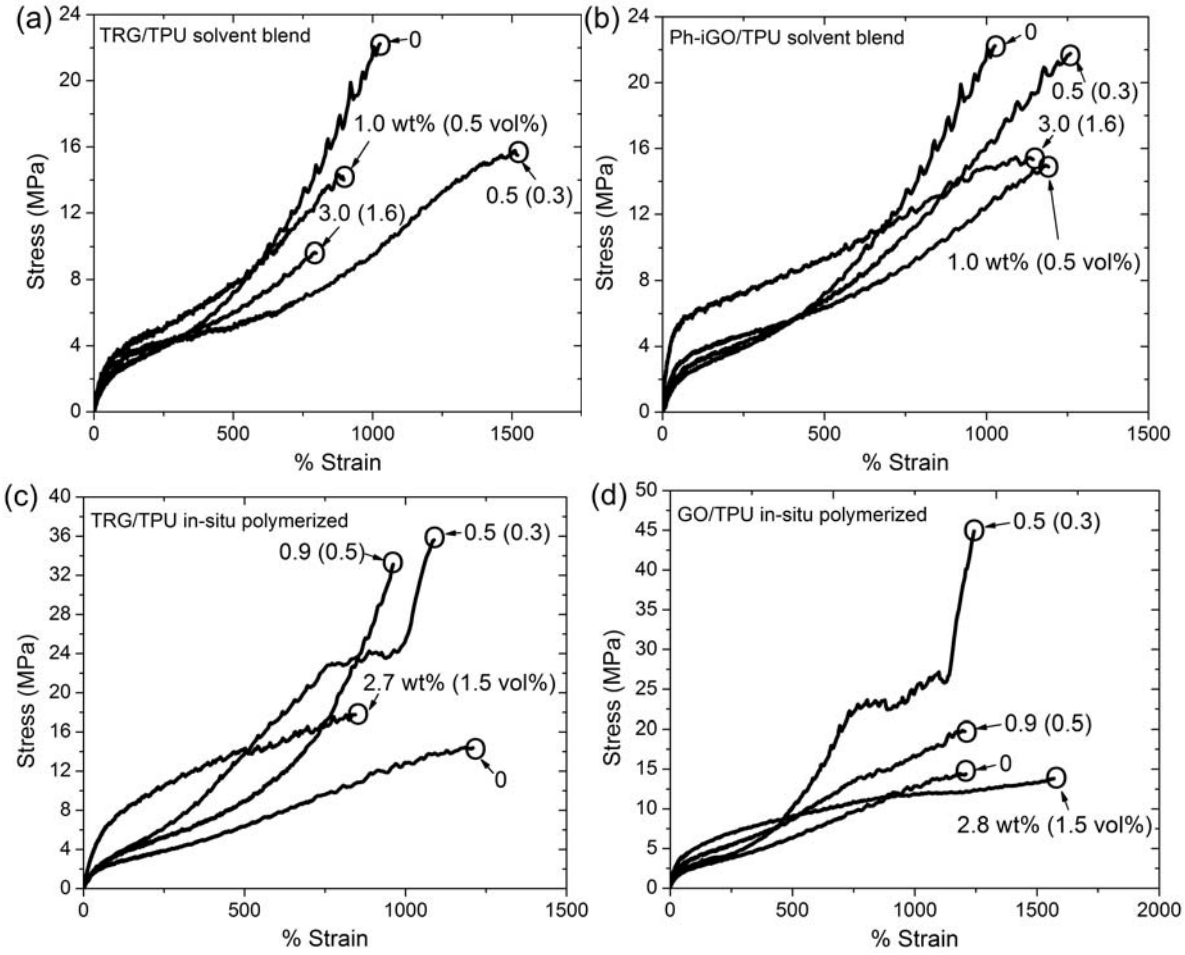

Figure SI8. Stress-strain responses of TPU reinforced with solvent mixed (a) TRG, (b) Ph-iGO and in-situ polymerized (c) TRG and (d) GO. The circled points mark sample failure and are labeled with wt% (vol%) of graphene. Note the difference in scales. The ultimate strength for in-situ polymerized TPU is 14 MPa versus 22 MPa for solvent blended Avalon 70AE.